J. Cell. Mol. Med. Vol 16, No 3, 2012 pp. 593-603

Antihyperglycaemic activity of 2,4:3,5-dibenzylidene-D-xylose-diethyl dithioacetal in diabetic mice

Arie Gruzman [a, #, §], Anna Elgart [b, #], Olga Viskind [a], Hana Billauer [c], Sharon Dotan [c], Guy Cohen [a], Eyal Mishani [c], Amnon Hoffman [b], Erol Cerasi [d], Shlomo Sasson [a, *]

[a] *Department of Pharmacology, Institute for Drug Research, School of Pharmacy, Faculty of Medicine, The Hebrew University of Jerusalem, Jerusalem, Israel*
[b] *Department of Pharmaceutics, Institute for Drug Research, School of Pharmacy, Faculty of Medicine, The Hebrew University of Jerusalem, Jerusalem, Israel*
[c] *Department of Nuclear Medicine, Hebrew University-Hadassah Medical Centre, Jerusalem, Israel*
[d] *Endocrinology and Metabolism Service, Department of Internal Medicine, Hebrew University-Hadassah Medical Centre, Jerusalem, Israel*

Received: February 22, 2011; Accepted: May 5, 2011

Abstract

We have recently generated lipophilic D-xylose derivatives that increase the rate of glucose uptake in cultured skeletal muscle cells in an AMP-activated protein kinase (AMPK)-dependent manner. The derivative 2,4:3,5-dibenzylidene-D-xylose-diethyl dithioacetal (EH-36) stimulated the rate of glucose transport by increasing the abundance of glucose transporter-4 in the plasma membrane of cultured myotubes. The present study aimed at investigating potential antihyperglycaemic effects of EH-36 in animal models of diabetes. Two animal models were treated subcutaneously with EH-36: streptozotocin-induced diabetes in C57BL/6 mice (a model of insulin-deficient type 1 diabetes), and spontaneously diabetic KKAy mice (Kuo Kondo rats carrying the A^y yellow obese gene; insulin-resistant type 2 diabetes). The *in vivo* biodistribution of glucose in control and treated mice was followed with the glucose analogue 2-deoxy-2-[^{18}F]-D-glucose; the rate of glucose uptake in excised soleus muscles was measured with [^{3}H]-2-deoxy-D-glucose. Pharmacokinetic parameters were determined by non-compartmental analysis of the *in vivo* data. The effective blood EH-36 concentration in treated animals was 2 μM. It reduced significantly the blood glucose levels in both types of diabetic mice and also corrected the typical compensatory hyperinsulinaemia of KKAy mice. EH-36 markedly increased glucose transport *in vivo* into skeletal muscle and heart, but not to adipose tissue. This stimulatory effect was mediated by Thr^{172}-phosphorylation in AMPK. Biochemical tests in treated animals and acute toxicological examinations showed that EH-36 was well tolerated and not toxic to the mice. These findings indicate that EH-36 is a promising prototype molecule for the development of novel antidiabetic drugs.

Keywords: AMPK • antihyperglycaemic drugs • D-xylose derivatives • diabetes • glucose transport • hyperglycaemia • KKAy mice

Introduction

Diabetes mellitus has become a worldwide epidemic and the estimated number of type 2 diabetic patients is expected to increase dramatically in the coming decades [1]. The aetiology of type 2 diabetes is associated with the development of insulin resistance, characterized by impeded capacity of peripheral tissues (*e.g.*, skeletal muscles) to utilize glucose effectively [2]. The resulting hyperglycaemia exacerbates this impairment by down-regulating the rate of glucose transport and utilization, most notably in skeletal muscles [3]. Antidiabetic drug therapy aims at restoring normal glucose homeostasis and thereby reducing the risk of late complications of the disease. However, mono- and even combination therapy with existing oral antihyperglycaemic drugs often fails to achieve stable normoglycaemia in diabetic patients, who eventually resort to insulin therapy [4]. Therefore, novel targets for

[#]These authors equally contributed to this work.
[§]Current address: Division of Medicinal Chemistry, Department of Chemistry, Faculty of Exact Sciences, Bar-Ilan University, Ramat Gan 52900, Israel.
*Correspondence to: Shlomo SASSON, Ph.D., Department of Pharmacology, School of Pharmacy, Faculty of Medicine, The Hebrew University, 91120 Jerusalem, Israel.
Tel.: +972-2-675-8798
Fax: +972-2-675-8741
E-mail: ShlomoSasson@huji.ac.il

doi:10.1111/j.1582-4934.2011.01340.x

antidiabetic drugs are sought; the enzyme AMP-activated protein kinase (AMPK) has emerged as a unique target because it induces glucose transporter-4 (GLUT-4) translocation from intracellular storage compartments to the plasma membrane of skeletal muscle in a non-insulin-dependent manner [5].

We have previously generated several lipophilic D-xylose derivatives that increased glucose uptake in cultured rat and human myotubes [6]. Among these, compound EH-36 (2,4:3,5-dibenzylidene-D-xylose-diethyldithioacetal) markedly enhanced glucose uptake in cultured myotubes by activating AMPK and inducing GLUT-4 translocation to the plasma membrane. In the present study we investigated whether these *in vitro* results could be reproduced *in vivo* in animal models of type 1 and type 2 diabetes.

Materials and methods

Materials

EH-36 was synthesized and purified as previously described [6]. Human recombinant insulin (Actrapid) was from Novo Nordisk (Bagsvaerd, Denmark). AICAR (5-aminoimidazole-4-carboxamide 1-β-D-ribofuranoside), anthrone, bovine serum albumin, (BSA, fraction V), cytochalasin B, 2-deoxy-D-glucose (dGlc), D-glucose, lecithin, peanut oil, polyoxyl 40-hydroxy castor oil, protease inhibitor cocktail, sesame oil, sodium citrate, Span 85, streptozotocin (STZ), trilaurin and Tween 20 were purchased from Sigma-Aldrich Chemicals (Rehovot, Israel). Glycerol and sodium fluoride were from Merck (Whitehouse Station, NJ, USA). Mercaptoethanol, phenylmethanesulfonyl fluoride, sodium orthovanadate, sodium-β-glycerophosphate, sodium pyrophosphate and sodium dodecyl sulphate were from Alfa Aesar (Ward Hill, MA, USA). American Radiolabeled Chemicals (St. Louis, MO, USA) supplied 2-[1,2–^{3}H]-deoxy-D-glucose ([^{3}H]dGlc; 2.22 TBq/mM [60 Ci/mM]). Anti-AMPK and anti-pThr^{172}-AMPK antibodies were from Cell Signaling Technology (Beverly, MD, USA). Horseradish peroxidase-conjugated anti-rabbit IgG and Easy Enhanced-chemoluminescence detection kit were from Jackson ImmunoResearch (West Grove, PA, USA). Organic solvents (high-performance liquid chromatography grade) were purchased from Frutarom Ltd. (Haifa, Israel).

Animals

Male Wistar rats (12 weeks old, 275–300 g) and C57BL/6 mice (7–8 weeks, 25–30 g) were purchased from Harlan Industries (Rehovot, Israel). The mice were made diabetic by two i.p. STZ injections (50 mg/kg body weight, in citrate buffer) with 1 week interval, as described [7]. Hyperglycaemic mice (5–10 per group, random blood glucose 15–25 mM) were used 2–4 weeks after the last injection. Diabetic male KKAy mice (3–5 per group, 8 to12 weeks old, 20–25 g) were purchased from Jackson Laboratory (Bar Harbor, ME, USA). Animals were routinely kept in 12 hr light/dark cycles and provided with chow and water *ad libitum*. Blood glucose levels at the time of killing ranged between 17 and 25 mM. The joint institutional animal care and use committee of the Hebrew University and Hadassah Medical Centre approved the study protocol for animal welfare. The Hebrew University is an AAALAC international accredited institution.

Preparation of EH-36 for s.c. and i.v. administration

The compound was dissolved in sesame oil at 60°C with extensive stirring to obtain a fine suspension for s.c. administration. EH-36 formulation for i.v. administration was prepared by the pre-concentrate preparation method [8]. Briefly, two mixtures were prepared: the first consisted of a suitable organic solvent and phospholipids (lecithin) at the ratio of 8:1; the second consisted of triglycerides (trilaurin), polyoxyl 40-hydroxy castor oil, Tween 20 and Span 80 at equal amounts. Each mixture was gently stirred and heated to 40°C until a homogenous solution was formed. Both mixtures were then added at 1:1 (v/v) ratio to 5 mg EH-36, and gently stirred and warmed at 40°C until a homogenous solution was formed. When mixed with water preheated to 37°C (1:9) and upon short (30 sec.) vortex mixing, this pre-concentrate mixture of EH-36 (0.5 mg/ml) spontaneously formed an encapsulated oil/water microemulsion suitable for i.v. injection.

Intraperitoneal glucose tolerance test (IP-GTT)

A standard IP-GTT test was performed on mice after an overnight fast. Glucose in saline was injected intraperitoneally (1.5 g/kg body weight). Venous blood samples from small tail clips were taken for glucose determination using a glucometer (FreeStyle Freedom; Abbott Diabetes Care, Alamada, CA, USA).

Preparation of soleus muscle lysates and Western blot analyses

Mice were killed with an i.p. injection of a lethal dose of ketamine-xylazole, soleus muscles were quickly excised, frozen in liquid nitrogen, weighed, pulverized, homogenized, centrifuged and the supernatant was collected as described [9]. The protein content in the supernatant was determined according to Bradford, using BSA standard dissolved in the same homogenization buffer. Polyacrylamide gel electrophoresis and Western blot analyses were performed with the indicated antibodies according to the antibody suppliers' protocols or to previously established protocols [6].

Glucose uptake assay in isolated mouse soleus muscles

Mice were killed, soleus muscles quickly isolated as described [3], and washed with glucose-free Krebs–Ringer bicarbonate (KRB) buffer (pH 7.4) under 95% O_2:5% CO_2 atmosphere. Insulin (100 nM) was added to muscles incubated with the same buffer, supplemented with 0.5% (w/v) BSA, for 20 min. prior to the uptake assay. Paired muscle incubations and uptake assays were performed: the right leg muscle received 30 μM of the glucose transporter inhibitor cytochalasin B prior to the uptake assay to determine non-carrier-mediated uptake, whereas the left leg muscle served to measure total uptake. Each muscle was incubated separately with 1.5 ml of the dGlc uptake solution [0.1 mM dGlc and 0.74 MBq/ml (20 μCi/ml) [^{3}H]dGlc in KRB buffer, pH 7.4] and incubated for 5 min. at 30°C under 95% O_2:5% CO_2 atmosphere with gentle shaking. The isolated muscles were then washed twice with 1.5 ml ice-cold stop solution (20 mM D-glucose, 1.2 mM Hg_2Cl_2 and 50 μM cytochalasin B in KRB buffer), blotted on filter papers, frozen in liquid nitrogen and weighed. The muscles were then solubilized in 1 ml of 1 M NaOH (15 hrs at 80°C), neutralized with

hydrochloric acid, mixed with 8 ml scintillation cocktail and counted in a β-scintillation counter. Non-carrier-mediated uptake ranged between 10% and 20% of the total dGlc uptake in the muscles.

In vivo 2-deoxy-2-[^{18}F]-D-glucose ([^{18}F]-FDG) biodistribution

[^{18}F]-FDG was prepared in the Cyclotron Unit at the Hebrew University-Hadassah Medical Centre in a TRACERlab MX FDG machine (General Electric, Waukesha, WI, USA) according to the manufacturer's protocol. The biodistribution of the radioactive tracer in mouse organs and tissues was determined in the Cyclotron Unit. Male C57BL/6 mice (7–8 weeks) received 0.962 MBq (26 μCi) of [^{18}F]-FDG by i.v. injection (in 100 μl saline) to the lateral tail vein. After 1 hr, a blood sample was drawn from the orbital sinus, the mice were killed by cervical dislocation and selected organs (soleus muscle, epididymal fat, heart, liver and pancreas) were excised, weighed and the radioactivity was measured in a 1480 WIZARD 3′ gamma counter (Waltham, MA, USA).

Glycogen determination

The glycogen content in hearts, livers and skeletal muscles isolated from mice was measured according to Roe and Dailey [10].

Determination of EH-36 level in mouse and rat plasma

Plasma samples (170 μl) were mixed with 225 μl acetonitrile and extracted with 4 ml ethyl acetate. The ethyl acetate phase was collected and evaporated to dryness in a vacuum evaporator and the residue reconstituted with 70 μl acetonitrile. EH-36 levels in the extracts were determined using an liquid chromatography-mass spectrometry system that comprised a 600S controller pump, a 717-plus Autosampler and a Micromass ZQ mass spectrometer (Waters Co., Milford, MA, USA). Briefly, 20 μl of the extracts were injected to the machine; the mobile phase was an acetonitrile:water (70:30) mixture containing 0.1% (v/v) formic acid. The flow rate was 0.25 ml/min. in a Waters XTerra C18 MS column (3.5 μm, 2.1 × 100 mm) at 35°C throughout the separation. Retention time for the internal standard talinolol was 6 min. The detection mass (*m/z*) was 455.2. The limit of quantification was 10 ng/ml.

Pharmacokinetic analyses

Rat studies: Rats were anesthetized for the period of surgery by i.p injection of 1 ml/kg 9:1 ketamine-xylazine solution, and maintained at 37°C on a heated surface (Harvard Apparatus, Inc., Holliston, MA, USA). An indwelling cannula was placed in the right jugular vein for systemic blood sampling as described [11]. This cannula was tunnelled beneath the skin and exteriorized at the dorsal part of the neck and used for i.v. administration and blood sampling. At the end of surgery animals were transferred to metabolic cages for a 12–18 hr recovery period with free access to water only. The microencapsulated formulation of EH-36 (5 mg/kg body weight) was administered to the animals by slow i.v. bolus injection. Chow was put in the cages 4 hrs after drug administration. Systemic blood samples (0.35 ml) were collected at 5 min. before treatment and at 2, 5, 15 and 30 min., and 1, 2, 3, 4 and 8 hrs thereafter; equal volumes of physiological solution were administered to the rats following each withdrawal of a blood sample. *Mouse studies*: EH-36 solution in sesame oil was prepared as described above and used for s.c. injections. The plasma levels of EH-36 were determined over a 48 hr period, during which the compound was administered to the mice at 0, 12, 14 and 36 hrs. The mice (three per group) were killed by cardiac puncture at zero time (prior to the first injection) and at 12, 24, 36 and 48 hrs during the treatment. The blood was collected in heparin-coated tubes. In both rat and mouse studies, plasma was separated by centrifugation and stored at –20°C until analysis. Non-compartmental pharmacokinetic analysis was performed with WinNonlin software, standard edition version 5.0.1 (Pharsight, Mountain View, CA USA). The concentration- and time-course data were analysed by the model-independent technique.

Serum insulin determination and blood biochemistry tests

Blood was collected by heart puncture and placed in heparin-washed test tubes. Plasma was separated by centrifugation. A 50 μl aliquot of each plasma sample was taken for insulin radioimmunoassay (suitable for rat and mouse insulin; Linco Research, St. Charles, MO, USA). The intra-assay coefficient of variation was 4–6% and the inter-assay coefficient of variation was 6–10%. The remaining plasma samples were analysed at the Clinical Biochemistry Department of The Hebrew University-Hadassah Medical Centre, per standard test cost.

Statistical analysis

Results are given as mean ± S.E.M. Statistical significance ($P < 0.05$) was calculated among experimental groups using the two-tailed Student's t-test.

Results

Blood-glucose lowering effect of EH-36

The structure of EH-36 is shown in the inset to Figure 1, which also shows the plasma levels attained in STZ-C57BL/6 mice following repeated four s.c. depot injections (at 12 hr intervals) of 10 mg/kg body weight. EH-36 was detectable in plasma after a 12 hr lag period; half-maximal and maximal plasma levels (1.1 and 2.1 μM, respectively) were reached at 22 and 36 hrs. Importantly, these plasma concentrations are comparable to the *in vitro* effective concentration of EH-36 reported before (5.0 μM; [6]).

The effect of EH-36 on blood glucose levels was evaluated following its s.c. injection (10 mg/kg of EH-36, twice a day) to STZ-treated C57BL/6 mice and KKAy diabetic mice. EH-36 demonstrated marked antihyperglycaemic activity: it significantly reduced blood glucose in STZ-treated C57BL/6 mice by 33% and 54% on days 3 and 4 of treatment, respectively, whereas oil

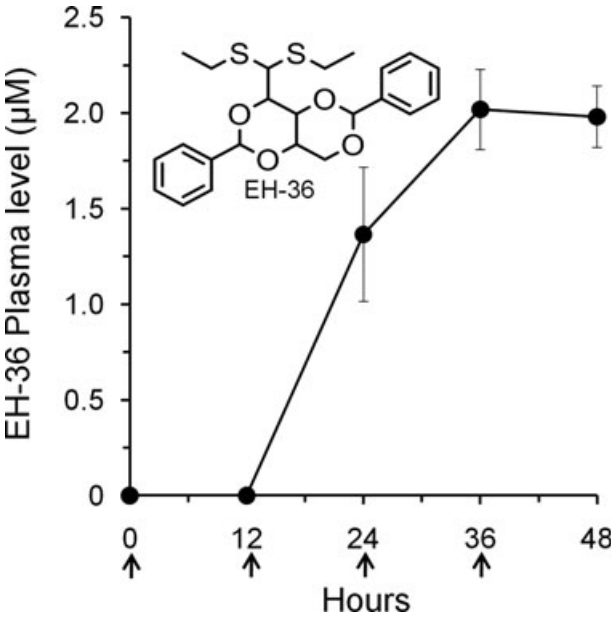

Fig. 1 Time-dependent increase of EH-36 in the plasma of male C57BL/6 mice. Mice were injected s.c. every 12 hrs for 2 days 10 mg EH-36/kg body weight. Plasma levels of EH-36 were determined at the indicated times, as described under Materials and methods. Mean ± S.E.M., $n = 3$. Inset: EH-36 structural formula. Arrows indicate injection times. Zero-time level was determined in naive animals. Mean ± S.E.M., $n = 3$.

treatment (vehicle) had no effect (Fig. 2A). EH-36 was even more effective in KKAy diabetic mice: blood glucose was reduced by 39%, 55% and 60% on days 2, 3 and 4 of treatment, respectively (Fig. 2B). Similar results were observed in these animals when the treatment was extended to 7 days. Yet, normoglycaemia was not attained in the diabetic mice following these 4- and 7 day treatments. In the rest of the experiment the mice were treated with EH-36 for 4 days to minimize the accumulation of oil at the sites of injection and to lower the risk of developing inflammatory reactions. In parallel with the reduction of blood glucose concentration, the KKAy mice, which are usually hyperinsulinaemic, became normoinsulinaemic during this treatment (Fig. 2C). The glucose-lowering effect of EH-36 was not restricted to diabetic animals: Figure 2D shows that it reduced blood glucose also by 20–25% in normoglycaemic control C57BL/6 mice.

The antihyperglycaemic effect of EH-36 was further explored with IP-GTT tests. Both types of diabetic mice were treated with sesame oil (150 μl) or EH-36 (10 mg/kg, s.c. twice daily) for 4 days, after which IP-GTT was performed at 9 a.m. after an overnight fast. The summaries of these data in absolute (Fig. 3A and C) and relative blood glucose levels (Fig. 3C and E) show a significant improvement in glucose tolerance in both mouse models following EH-36 treatment. Figure 3C and F shows the corresponding area under the curve (AUC) values: 1156 ± 231 *versus* 627 ± 162 mmol of glucose/l · min. for oil- and EH-36-treated STZ-C57BL/6 mice, respectively; and 1380 ± 257 *versus* 950 ± 141 for the respective

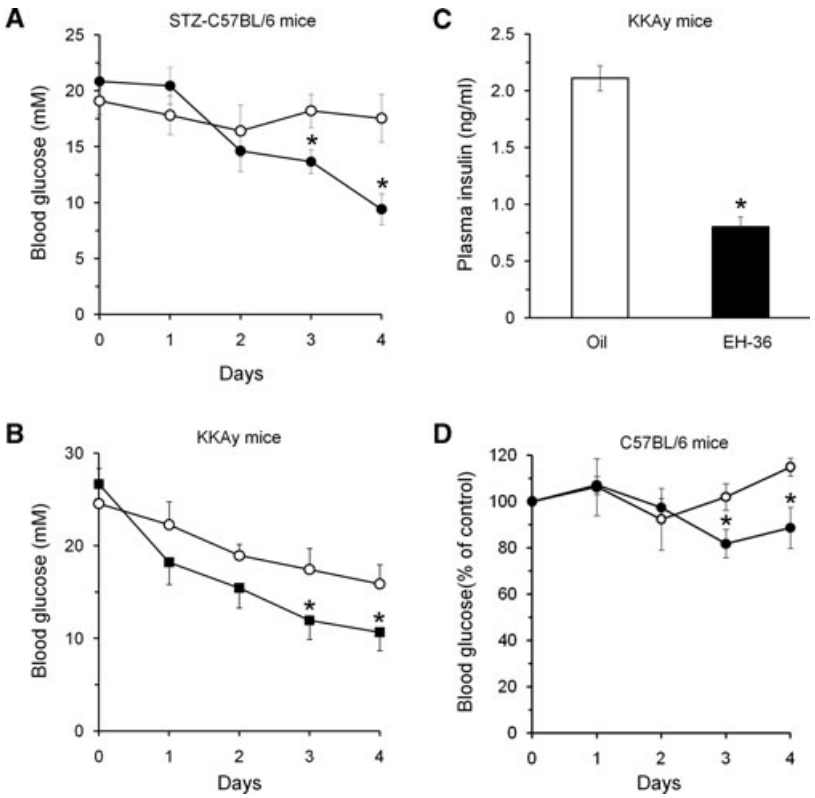

Fig. 2 Antihyperglycaemic effects of EH-36 in STZ-C57BL/6 and KKAy diabetic mice. (**A**) STZ-C57BL/6 mice were injected s.c. twice daily for 4 days 10 mg EH-36/kg body weight (black circles) or 150 μl sesame oil (open circles). Blood glucose levels were determined at the indicated times. (**B**) KKAy mice were similarly treated with EH-36 (black squares) or the vehicle (open squares). (**C**) Plasma insulin levels were determined in samples taken from the EH-36- and oil-treated KKAy mice described in (**B**). (**D**) Normal (non-diabetic) C57BL/6 mice were treated with EH-36 or oil as described above. The blood glucose levels at day zero were 7.8 ± 0.6 and 7.6 ± 0.9 mM for the control and EH-36 treated group, respectively. Mean ± S.E.M., $n = 5$–10, $^*P < 0.05$ in comparison with the oil-treated groups.

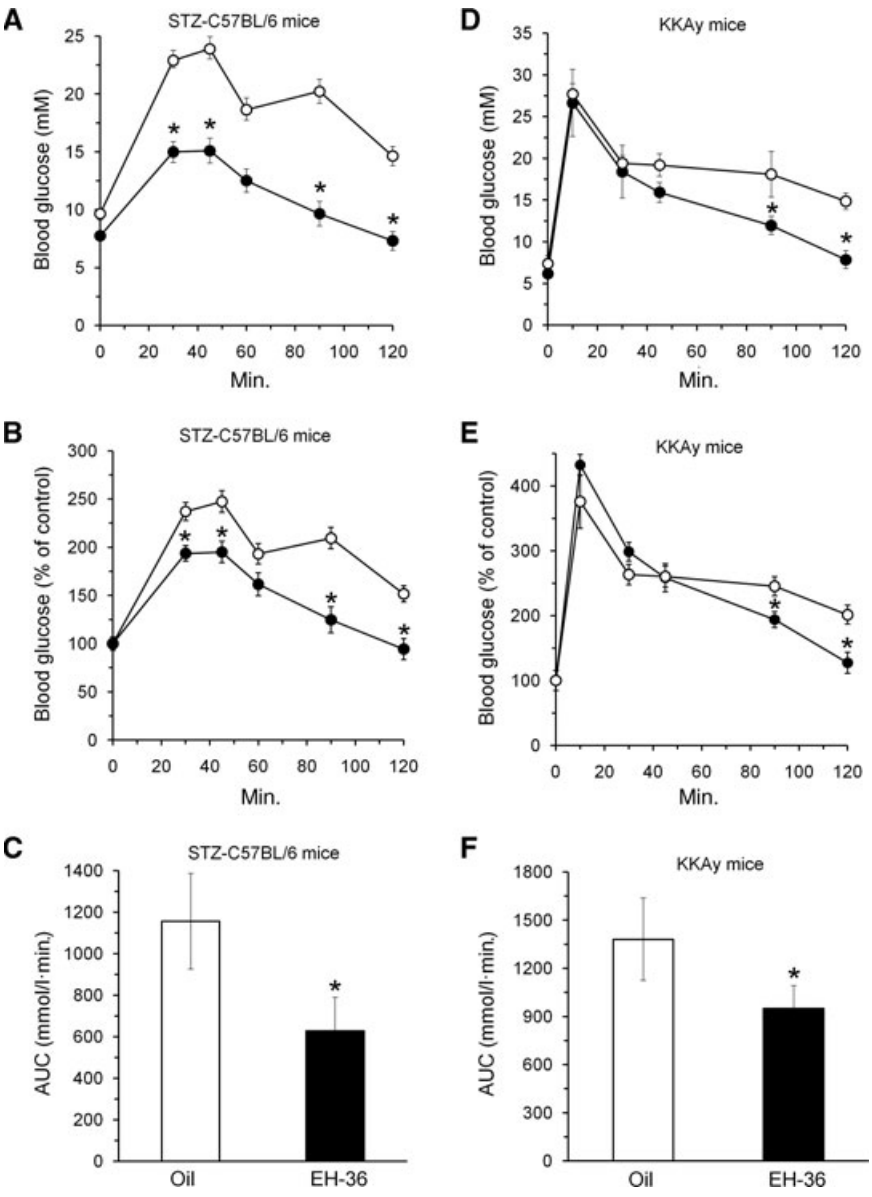

Fig. 3 EH-36 improves glucose tolerance in STZ-C57BL/6 and KKAy diabetic mice. The mice were treated with EH-36 or oil as described in the Figure 2A legend. Following overnight fast they were taken in the morning for an IP-GTT, as described under Materials and methods. (**A**) and (**B**) Summary of tests performed on oil- (open circles) and EH-36-treated STZ-C57BL/6 mice (black circles). (**C**) Average AUC values of the individual IP-GTT tests shown in (**A**). (**D**) and (**E**) Summary of tests performed on oil- (open squares) and EH-36-treated KKAy diabetic mice. (**F**) AUC values of the individual IP-GTT tests shown in (**C**). Mean ± S.E.M., $n = 5–10$, $^*P < 0.05$ in comparison with the oil-treated group.

KKAy mice. These results indicate that EH-36 improved total body glucose disposal by 30–50% following 4 days of treatment.

EH-36 improves the glucose uptake of skeletal muscles in diabetic mice

The capacity of EH-36 to augment peripheral glucose disposal in STZ-C57BL/6 mice was then determined by measuring the biodistribution of the non-metabolized radioactive tracer [^{18}F]-FDG. Figure 4A and B shows a significant increase in the accumulation of the radioactive glucose analogue in soleus muscles and hearts isolated from EH-36-treated mice in comparison with the organs removed from oil-treated control mice. These differences remain significant whether the accumulation was calculated as a percentage of the injected dose of [^{18}F]-FDG per tissue weight (Fig. 4A) or as the tissue to blood ratio of [^{18}F]-FDG (Fig. 4B). Noteworthy, no significant accumulation of [^{18}F]-FDG was found in the epididymal fat, liver and pancreas of EH-36-treated mice in comparison with the control group.

We then employed an *ex vivo* assay to measure the [^{3}H]-dGlc uptake capacity of soleus muscles isolated from oil- or EH-36-treated diabetic STZ-C57BL/6 mice (Fig. 5A) and KKAy mice (Fig. 5B). In both models, the rate of uptake was over 2-fold higher in muscle from the EH-36-treated mice in comparison with the oil-treated control mice. Notably, the 4 day of the *in vivo* treatment

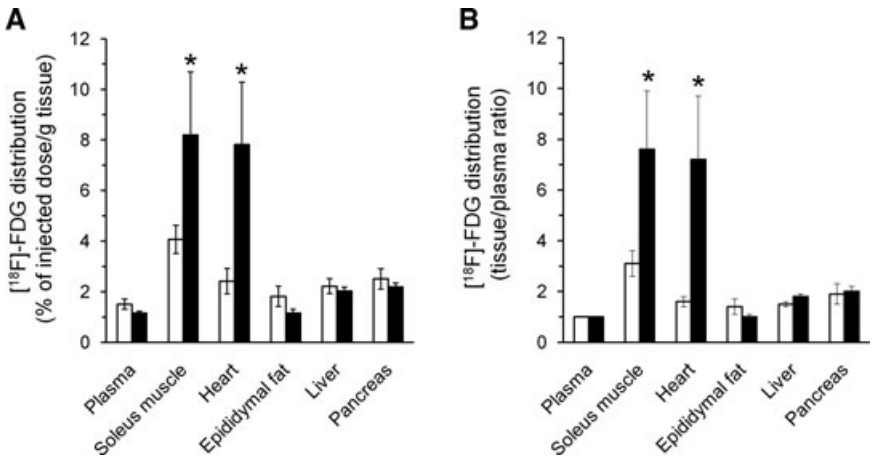

Fig. 4 Biodistribution of [^{18}F]-FDG in organs of EH-36-treated STZ-C57BL/6 mice. The mice were treated with EH-36 (black bars) or oil (open bars) as described in the Figure 2A legend. On the morning of day 5 they received an i.v. injection of [^{18}F]-FDG and were further processed, as described under Materials and methods. (**A**) Distribution of the radioisotope was calculated as the percentage of the injected dose per gram of organ. (**B**) The tissue-to-plasma ratio of the isotope was calculated by dividing the radioactivity in 1 g tissue by the radioactivity in 1 g plasma. Mean ± S.E.M., $n = 5–10$, $^*P < 0.05$ in comparison with the oil-treated mice.

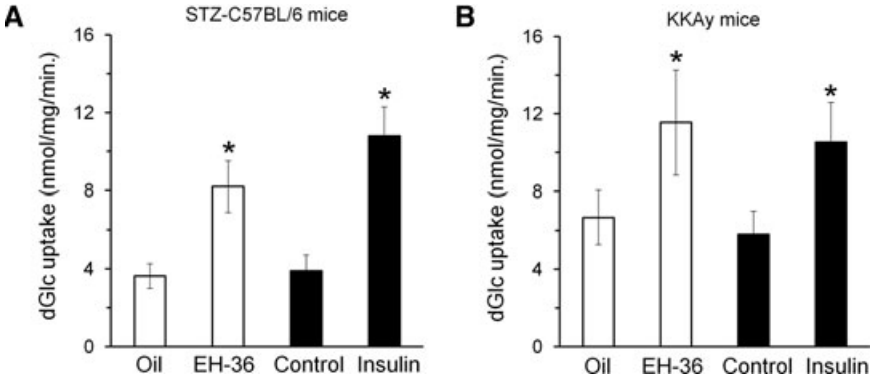

Fig. 5 Effect of EH-36 treatments and of *in vitro* insulin on dGlc uptake in isolated soleus muscles. STZ-C57BL/6 (**A**) and KKAy diabetic mice (**B**) were treated with EH-36 or oil as described in the Figure 2 legend. Soleus muscles were isolated from the mice on day 5 and incubated for *in vitro* [^{3}H]dGlc uptake, as described under Materials and methods. Soleus muscles isolated from untreated STZ-C57BL/6 and KKAy diabetic mice were incubated with 100 nM insulin for 20 min. prior to the uptake assay, as described under Materials and methods. Mean ± S.E.M., $n = 5–10$, $^*P < 0.05$ in comparison with respective controls.

with EH-36 appears as effective as the short-term *in vitro* addition of insulin in augmenting the rate of glucose uptake in the muscles of these mouse models of type 1 and type 2 diabetes.

EH-36 induces *in vivo* Thr^{172} phosphorylation of AMPK in skeletal muscle

We have previously shown that EH-36 *in vitro* induces translocation of GLUT-4 to the plasma membrane of L6 myotubes in an AMPK-dependent manner [6]. To investigate whether EH-36 operates by this mechanism also *in vivo*, we treated STZ-C57BL/6 and KKAy mice with EH-36 or oil for 4 days, excised their soleus muscles and determined the extent of Thr^{172} phosphorylation in AMPK. AICAR, the pharmacological activator of AMPK (added at 4 mM for 30 min. to muscles isolated from naive mice) served as a positive control. Figure 6A–D depicts that Thr^{172}-AMPK phosphorylation was 1.85- and 1.76-fold higher in muscles isolated from EH-36 treated STZ-C57BL/6 and KKAy mice, respectively, in comparison with the respective oil-treated controls. The total muscle content of AMPK was not altered. Of note, the level of AMPK phosphorylation in the liver of both types of mice remained unaltered following EH-36 treatment (data not shown).

Pharmacokinetic analysis

The pharmacokinetic parameters of EH-36 were determined in rats as described under Materials and methods. Figure 7 depicts the temporal changes in the plasma concentration of EH-36 after a single i.v. bolus injection. The compound was cleared from the plasma with a $T_{1/2}$ of 21.7 ± 1.7 min. Other pharmacokinetic parameters of EH-36 are given in Table 1. The value of EH-36 plasma protein binding capacity, shown in this table, is taken from our previous study [6].

Liver and renal function and plasma lipid profile in EH-36-treated mice

STZ-C57BL/6 mice and KKAy mice were treated with EH-36 or oil for 4 days as described above. The glycogen content in quadriceps muscles and hearts of EH-36-treated C57BL/6- and KKAy mice remained comparable to that measured in the organs isolated from the respective oil-treated controls (Table 2). Yet, there was a ~50% reduction in KKAy liver glycogen content following the treatment with EH-36, while hepatic glycogen content in C57BL/6 mice was not affected.

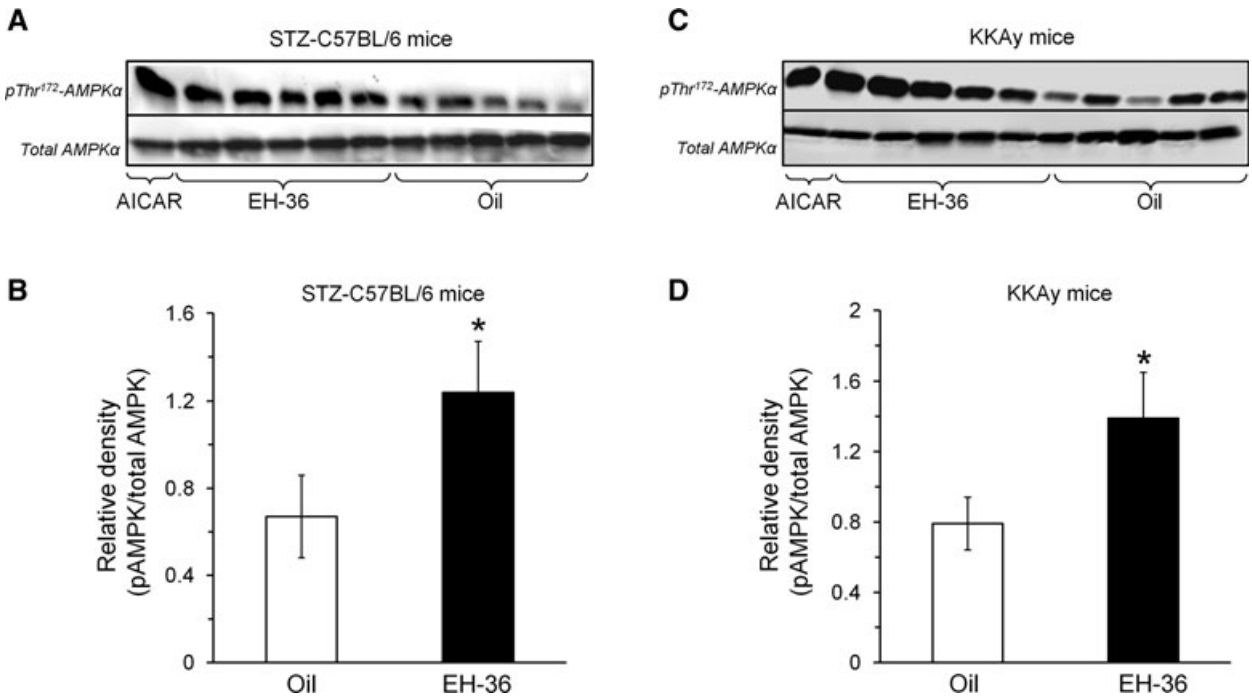

Fig. 6 EH-36 activates AMPK in soleus muscles of STZ-C57BL/6 and KKAy diabetic mice. STZ-C57BL/6 (**A**, **B**) and KKAy diabetic mice (**C**, **D**) were treated with EH-36 or oil as described in the Figure 2A legend. Soleus muscles were isolated from the mice on day 5 and processed for AMPK and pThr^{172}AMPK Western blot analysis as described under Materials and methods. AICAR (4 mM) was added for 30 min. to soleus muscles isolated from untreated animals. (**A**) and (**C**) show representative Western blots; (**B**) and (**D**) give the summary of band densities of 3 independent experiments (open bars: control mice, black bars: EH-36 treated mice). Mean ± S.E.M., $n = 3$, $^*P < 0.05$ in comparison with respective oil controls.

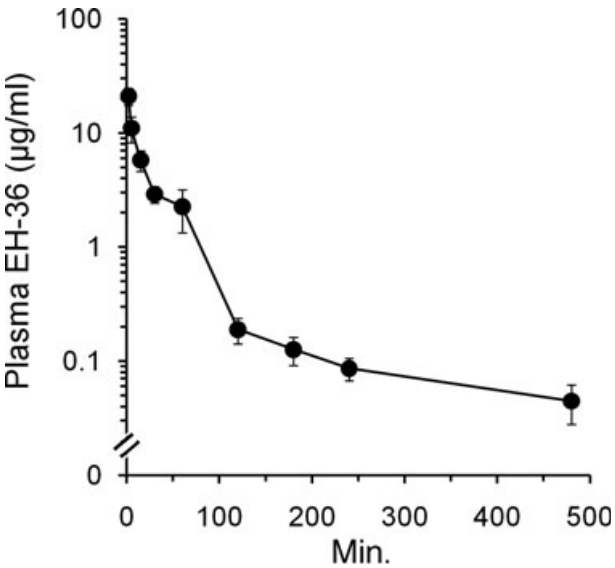

Fig. 7 Time-course analysis of plasma levels of EH-36. The formulation of EH-36 for an i.v. injection is described under Materials and methods. Non-diabetic Wistar rats received EH-36 (5 mg/kg body weight) by a single i.v. bolus injection. Blood samples were drawn at the indicated times and taken for extraction and GC-MS analysis of EH-36, as described under Materials and methods. Mean ± S.E.M., $n = 3$.

Table 1 Pharmacokinetic parameters of EH-36

PK parameters	Value
$T_{1/2}$ (min.)	21.7 ± 1.7
AUC (μM/min.)	83.0 ± 21.1
Vd (l/kg body weight)	2.4 ± 0.1
CL (ml/min./kg body weight)	83.3 ± 2.6
C_{max} (μM)	2.8 ± 0.4

The pharmacokinetic parameters of EH-36 were determined following a single bolus injection to rats, as described under Materials and methods. Mean ± S.E.M., $n = 3$.

Table 3 shows that serum triglycerides and total cholesterol in the EH-36-treated mice were not significantly different from oil-treated controls. The creatinine level in EH-treated diabetic KKAy mice was normal, but it was significantly increased in EH-36 treated STZ-C57BL/6 mice. Liver function, as determined by the activities of alanine transaminase, alkaline phosphatase, γ-glutamyl transferase and aspartate aminotransferase remained unaltered in EH-36-treated mice.

Table 2 Glycogen content in quadriceps muscles, hearts and livers of oil- and EH-36 treated STZ-C57BL/6 and KKAy mice

Mouse model:	**STZ-C57BL/6 mice**		**KKAy mice**	
Treatment:	**Oil**	**EH-36**	**Oil**	**EH-36**
Quadriceps muscle	0.23 ± 0.24	0.21 ± 0.4	1.35 ± 0.23	1.34± 0.52
Heart	0.19 ± 0.02	0.21 ± 0.5	0.36 ± 0.04	0.39 ± 0.08
Liver	1.56 ± 0.09	1.29 ± 0.09	12.15 ± 1.23	6.17 ± 0.76*

STZ-C57BL/6 and KKAy mice were treated s.c. with EH-36 or oil as described in the Figure 2A legend. The organs were excised from mice after injection of a lethal dose of ketamine/xylasine. Glycogen content in the various organs was determined as described under Materials and methods. Results are given as μg glycogen/mg wet weight. Mean ± S.E.M., $n = 10$. *$P < 0.05$ significantly different from the respective oil-treated control mice.

Table 3 Blood biochemistry of oil- and EH-36 treated STZ-C57BL/6 and KKAy mice

	Normal C57BL/6 mice	**Oil-treated STZ-C57BL/6 mice**	**EH-36-treated STZ-C57BL/6 mice**	**Oil-treated KKAy mice**	**EH-36-treated KKAy mice**
Blood glucose (mM)	6.3 ± 0.4	19.7 ± 3.1*	8.3 ± 3.8	27.1 ± 4.8	13.6 ± 2.3*
Triglycerides (mM)	0.66 ± 0.12	0.7 ± 0.08	0.63 ± 0.09	1.43 ± 0.2	1.23± 0.34
Cholesterol (mM)	2.9 ± 0.2	2.5 ± 0.2	2.63 ± 0.28	2.33 ± 0.31	2.2 ± 0.1
Creatinine (μM)	83.2 ± 12.5	137.8 ± 14.9*	246.2 ± 21.0*	52.5 ± 3.5	43.3 ± 5.5
Alanine transaminase (U/l)	88.5 ± 5.2	116.6 ± 11.8	88.5 ± 14.4	54 ± 3.6	47 ± 6.3
Alkaline phosphatase (U/l)	<10	<10	<10	<10	<10
γ-glutamyl transferase (U/l)	76.6 ± 5.7	75.2 ± 8.4	64.2 ± 6.8	12.6 ± 2.8	10.6 ± 1.9
Aspartate aminotransferase (U/l)	225 ± 23	216 ± 41	256 ± 19	201 ± 15	279 ± 21.6

STZ-C57BL/6 and KKAy mice were treated with EH-36 or oil as described in the Figure 2A legend. Blood was collected, plasma separated and taken for biochemical analysis, as described under Materials and methods. Mean ± S.E.M., $n = 10$. *$P < 0.05$ significantly different from the respective oil-treated control mice.

Acute toxicology

A preliminary acute toxicology survey of EH-36 in mice was conducted by The Pre-clinical group Vetgenerics (Rehovot, Israel). EH-36 in sesame oil (50 mg/kg; dose volume: 3.3 ml/kg) or the vehicle were injected s.c. twice daily for 14 days to male and female C57BL/6J (20–22 g) control mice. No animal died and no pathological symptoms were detected during the injection period and a 2 week recovery period. The thoracic and abdominal cavities were exposed at the end of the survey: no abnormality in organ location, colour, shape or size was observed, except in one EH-36-treated male mouse where the spleen was partially dark.

Interestingly, body weight gain in the EH-36-treated male mice was significantly lower in comparison with the oil-treated animals throughout the injection period and the 2 weeks of recovery (Fig. 8). Nonetheless, the mean daily food consumption of these mice was not significantly different from that of the control group (2.35 ± 0.05 and 2.55 ± 0.15 g/day for EH-36-treated mice during the treatment and the recovery periods, respectively, *versus* 2.67 ± 0.11 and 2.65 ± 0.15 g/day for the oil-treated mice). Daily food consumption and body weight gain in female mice was similar with EH-36 or oil treatment throughout the injection and recovery periods.

Discussion

This study shows that low molecular weight lipophilic D-xylose derivatives may represent a new class of antihyperglycaemic compounds. The prototype molecule EH-36 reduced significantly

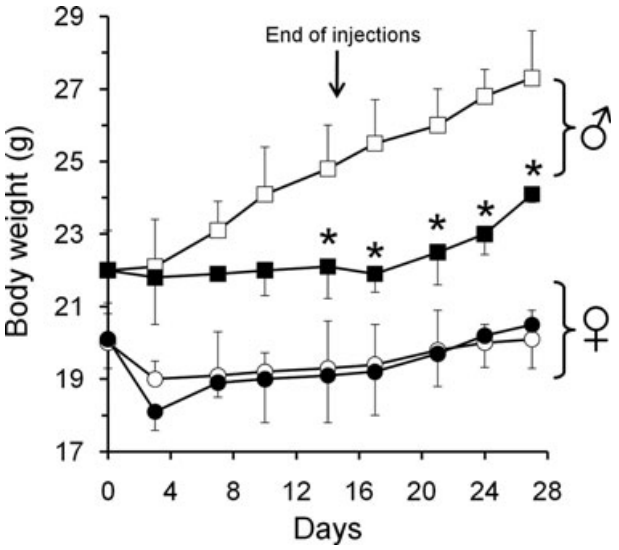

Fig. 8 EH-36 reduces body weight gain in male C57BL/6 mice. Non-diabetic male (squares) and female (circles) C57BL/6 mice were treated with EH-36 (50 mg/kg body weight; black symbols) or the vehicle (3.3 ml sesame oil/kg body weight; open symbols) once a day by s.c. injection for 14 days. A recovery period lasted for additional 2 weeks. Mean ± S.E.M., $n = 5$, $^*P < 0.05$ in comparison with the oil-treated male mice.

blood glucose in mouse models of type 1 (STZ-C57BL/6 mice) and type 2 diabetes (KKAy mice), but did not establish normoglycaemia. Of interest is the reduced sensitivity of KKAy mice to EH-36 blood glucose lowering effects in comparison with STZ-C57BL/6 mice. Two critical factors may explain this observation:

First, a decreased expression of GLUT-4 in skeletal muscles in hyperglycaemic KKAy mice in comparison with the non-diabetic wild-type mice [12]. Second, STZ-induced liver damage in STZ-C57BL/6 mice [13] could slow the hepatic metabolism of EH-36 and extend its biological effects.

A dose–response analysis of s.c. injected EH-36 showed similar blood glucose lowering effects up to 100 mg/kg body weight (data not shown). This is explained pharmacokinetically by a non-linear relationship in the release of lipophilic drugs from sesame oil depots [14]. Noteworthy, higher doses (*i.e.*, 300 mg/kg body weight) induced hypoglycaemia and high mortality of the treated mice within 7 days of injections. Due to the limited solubility of EH-36 even in oil, this dose escalation was accompanied with larger volumes of oil injected. This treatment caused noticeable inflammatory reactions and tissue damage at the sites of injection, which could increase the absorption of the drug and lead to hypoglycaemia.

Along with its antihyperglycaemic effect, EH-36 also attenuated the compensatory hyperinsulinaemia, which usually results from peripheral insulin resistance, in the type 2 diabetes model. Concomitantly, EH-36 augmented glucose uptake in skeletal muscle and heart, but not in adipose tissue and liver in both mouse models. The augmenting effect of EH-36 is correlated to the activation of AMPKα in skeletal muscle, but not in liver. In previous studies on cultured L6 myotubes we showed that EH-36 increased GLUT-4 abundance in the plasma membrane fraction in an AMPK-dependent manner, without engaging the insulin transduction mechanism in the process [6]. Interestingly, the efficacy of EH-36 in augmenting the rate of glucose uptake in skeletal muscle of the treated mice was comparable to the maximal *in vitro* stimulatory effect of insulin. However, although insulin has a rapid effect on muscle glucose uptake (20 min. exposure *in vitro*), the time course of the EH-36 effect (24–36 hr treatment in mice) is strikingly different. Insulin binds to its receptor and activates the transduction mechanism and promptly induces the translocation of GLUT-4-containing vesicles to the plasma membrane [15], However, a 24–36 hr lag period is required for EH-36 to reach an effective concentration *in vivo* (Fig. 1). We also compared the effect of EH-36 to the sulphonylurea derivative glibenclamide and found comparable blood glucose lowering activities for both; however, the onset of the effect of the former was faster than that of EH-36 (data not shown).

AMPK is a master regulator of cellular energy balance and is considered to be a key switch for glucose and lipid metabolism in various organs: in skeletal muscle it stimulates glucose transport and fatty acid oxidation; in the liver it augments fatty acid oxidation and decreases glucose output and cholesterol and triglyceride synthesis [16]. The AMPK complex consists of a catalytic α subunit and two regulatory subunits, β and γ. Various isoforms of these subunits are encoded by different genes and expressed in a tissue-specific manner. The α_2 subunit, which is the predominant catalytic AMPK subunit in skeletal muscle, is activated by Thr^{172} phosphorylation by various kinases [*i.e.*, serine/threonine protein kinase coded in the lkb locus (LKB1), transforming growth factor-β-activated kinase (TAK1) and calmodulin-dependent protein kinase kinase β (CaMKKβ)] [16–19]. The present study shows that systemic administration of EH-36 resulted in marked AMPKα Thr^{172} phosphorylation in skeletal muscle in both types of diabetic mice.

The activation of AMPK by Thr^{172} phosphorylation in contracting skeletal muscles, or following hypoxia, hyperosmolar shock or treatment with mitochondrial uncouplers and electron transport inhibitors, has been associated with relative energy depletion and increased AMP/ATP ratio [20]. The activated AMPK complex subsequently phosphorylates the protein AS160 at Thr^{642}, which then releases GLUT-4-containg vesicles from intracellular compartments and promotes their translocation to the plasma membrane [21, 22]. However, AMPK-independent mechanisms have also been suggested to mediate the effect of muscle contraction on glucose transport [23]. Nonetheless, mitochondrial dysfunction and impaired lipid metabolism in skeletal muscle of insulin resistant and type-2 diabetic patients have recently been linked to impaired AMPK activation [24]. AMPK shows cardioprotective effects, which have been attributed to augmented glucose transport and glycolysis in ischemic hearts [25, 26]. Indeed, post-ischemic cardiac damage was more severe in mice bearing a dominant-negative AMPKα_2 transgene in their cardiomyocytes [27].

The biguanide derivative metformin is a commonly prescribed antidiabetic drug, which primarily reduces hepatic glucose output, possibly by inhibiting complex I in the mitochondrion and increasing the cellular AMP/ATP ratio. Recent studies suggest that metformin also acts by activating AMPK in the liver [28]. The effect of metformin on skeletal muscle glucose metabolism is less clear. It has been suggested that metformin augments Rab4 expression in an AMPK-dependent manner, and that the former modulates insulin-mediated GLUT-4 translocation to the plasma membrane [29]. Others have found that metformin augments glucose uptake in L6 myotubes by pyruvate dehydrogenase kinase 1 (PDK1)-dependent activation of atypical PKC [30]. Nonetheless, improved insulin signalling by metformin-mediated reduction of inhibitor of nuclear factor κ-β kinase-β (IKKβ) activity in skeletal muscle has also been reported [31], as well as metformin-induced muscle mitochondrial dysfunction [32]. In contrast to these inconsistent reports on the role of AMPK in transducing the peripheral effects of metformin, EH-36 stands as a potent activator of AMPK in skeletal muscle. Based on our previous study in L6 myotubes [6], it appears that EH-36 recruits GLUT-4 to the plasma membrane of skeletal muscles by activating the AMPK-AS160 arm of the GLUT-4 translocation machinery.

The present *in vivo* and *ex vivo* analyses of skeletal muscles show that EH-36 stimulated primarily the glucose transport system in a non-insulin-dependent manner whereas glucose uptake in adipose tissues and livers was not affected. The antihyperglycaemic effect of EH-36 in STZ-C57BL/6 mice, in which the β-cell mass is dramatically reduced, indicates that the primary site of action of EH-36 is extra-pancreatic. Noteworthy, EH-36 had no noticeable effect on basal and glucose-stimulated insulin secretion from cultured INS-1E β-cells (data not shown). KKAy mice develop hyperinsulinaemia in early adulthood due to peripheral insulin resistance [33, 34]. The hyperglycaemia and hyperinsulinaemia of this mouse model (27.1 ± 4.8 mM and 2.1 ± 0.1 ng/ml, respectively) were significantly reduced following a 4 day treatment with EH-36 to 13.6 ± 2.3 mM and 0.8 ± 0.1 ng/ml, respectively. We attribute the reduction in plasma insulin to an improved peripheral glucose disposal and alleviation of the insulin resistant state.

The effective concentration of EH-36 in plasma (2 μM) is somewhat lower than the *in vitro* minimal effective concentration (5 μM) that we reported for cultured L6 myotubes [6]. The high values of the oil/water partition coefficient ($\log P = 4.99$), protein binding capacity (98.0 ± 0.3%) [6], and volume of distribution (Vd = 2.4 ± 0.1 l/kg body weight) of EH-36 reflect its strong lipophilic nature. This is closely associated with the sustained plasma level of EH-36 that we found in mice during depot administration (repeated s.c injections in oil suspension; Fig. 1). The short half-life of EH-36 demonstrated in the present report agrees with the calculated clearance rate. The *in vivo* metabolism and elimination EH-36 have not been yet fully studied. We prepared various EH-36 formulations for oral administration and tested them *in vivo* by oral (gavage) administration and *in vitro* in the CaCo-2 monolayer permeability model system: in both cases we could not find evidence of substantial EH-36 permeation through enterocytes in the gastrointestinal wall. Advanced formulations and/or derivatization of EH-36 will be required to improve its bioavailability and first-pass metabolism for effective oral administration.

We made a preliminary assessment of the safety of EH-36. Kidney and liver function in EH-36-treated KKAy mice was not modified. EH-36 reduced markedly liver glycogen accumulation in KKAy mice, which is in accordance with the reduced glucose and insulin levels in blood, resulting in lower glucose availability and glycogen synthase activity. In contrast, liver glycogen levels were not reduced in EH-36-treated STZ-C57BL/6 mice, whereas blood creatinine was increased. These observations most likely reflect long-term STZ-induced hepatotoxicity and nephrotoxicity in mice [13, 35, 36]. Nonetheless, total cholesterol and triglyceride levels were not significantly changed following EH-36 treatment of STZ-C57BL/6 and KKAy mice.

The reduced weight gain of EH-36-treated non-diabetic male C57BL/6 mice is interesting and surprising, because this was not observed in female mice. Whether additional targets for EH-36 that control energy expenditure or substrate futile cycling exist in male mice remains to be investigated. All in all, this preliminary examination suggests that EH-36 is not toxic in mice.

In summary, these *in vivo* findings and our previous study on the *in vitro* mechanism of action of EH-36 highlight the potential of such lipophilic D-xylose derivatives to form the basis of a new class of antihyperglycaemic agents. By activating AMPK specifically in skeletal muscles, these compounds ameliorate peripheral insulin resistance. Consequently, the peripheral demand for insulin is reduced, preventing the deterioration of β-cells, which is a characteristic finding in type 2 diabetes. Ongoing work focuses on EH-36 as a prototype molecule for the development of such novel oral antidiabetic drugs.

Acknowledgements

This study was supported by Diab R&D (France) and grants from the Applied Research Program A of the Hebrew University, The Deutch Foundation for Applied Sciences of the Hebrew University, Alex Grass Center for Drug Design and Synthesis of Novel Therapeutics, David R. Bloom Center for Pharmacy at the Hebrew University School of Pharmacy, the Nophar Program of the Israel Ministry of Commerce and Trade and the Israel Science Foundation of The Israel Academy of Sciences and Humanities. S.S. and A.H. are members of the David R. Bloom Center for Pharmacy at the Hebrew University of Jerusalem. A.G. and G.C. received fellowships from the Hebrew University Center for Diabetes Research. We thank G. Babai for performing the insulin radioimmunoassay. The pharmacokinetic analysis in this work is part of A.E's doctoral work.

Conflict of interest

The authors state no conflict of interest.

References

1. **Wild S, Roglic G, Green A, *et al.*** Global prevalence of diabetes: estimates for the year 2000 and projections for 2030. *Diabetes Care*. 2004; 27: 1047–53.
2. **Zierath JR, Kawano Y.** The effect of hyperglycaemia on glucose disposal and insulin signal transduction in skeletal muscle. *Best Pract Res Clin Endocrinol Metab*. 2003; 17: 385–98.
3. **Sasson S, Edelson D, Cerasi E.** *In vitro* autoregulation of glucose utilization in rat soleus muscle. *Diabetes*. 1987; 36: 1041–6.
4. **Ben Yakir M, Gruzman A, Alpert E, *et al.*** Glucose transport regulators. *Curr Med Chem: Immunol, Endocr Metab Agents*. 2005; 5: 519–27.
5. **Misra P.** AMP activated protein kinase: a next generation target for total metabolic control. *Expert Opin Ther Targets*. 2008; 12: 91–100.
6. **Gruzman A, Shamni O, Ben Yakir M, *et al.*** Novel D-xylose derivatives stimulate muscle glucose uptake by activating AMP-activated protein kinase alpha. *J Med Chem*. 2008; 51: 8096–108.
7. **Cossel L, Schneider E, Kuttler B, *et al.*** Low dose streptozotocin induced diabetes in mice. Metabolic, light microscopical, histochemical, immunofluorescence microscopical, electron microscopical and morphometrical findings. *Exp Clin Endocrinol*. 1985; 85: 7–26.
8. **Bekerman T, Golenser J, Domb A.** Cyclosporin nanoparticulate lipospheres for oral administration. *J Pharm Sci*. 2004; 93: 1264–70.
9. **Parvaresh KC, Huber AM, Brochin RL, *et al.*** Acute vascular endothelial growth factor expression during hypertrophy is muscle phenotype specific and localizes as a striated pattern within fibres. *Exp Physiol*. 2010; 95: 1098–106.
10. **Roe JH, Dailey RE.** Determination of glycogen with the anthrone reagent. *Anal Biochem*. 1966; 15: 245–50.
11. **Hoffman A, Levy G.** Kinetics of drug action in disease states. XXIX. Effect of experimental nephrotic syndrome on the pharmacodynamics of heptabarbital: implications of severe hypoalbuminemia. *J Pharmacol Exp Ther*. 1989; 249: 117–22.
12. **Kato M, Suwa A, Shimokawa T.** Glucose catabolic gene mRNA levels in skeletal muscle exhibit non-coordinate expression in hyperglycemic mice. *Horm Metab Res*. 2004; 36: 513–8.
13. **Carnovale CE, Marinelli RA, Rodriguez Garay EA.** Toxic effect of streptozotocin on the biliary secretion of nicotinamide-treated rats. *Toxicol Lett*. 1987; 36: 259–65.
14. **Larsen DH, Fredholt K, Larsen C.** Assessment of rate of drug release from oil vehicle using a rotating dialysis cell. *Eur J Pharm Sci*. 2000; 11: 223–9.
15. **Klip A.** The many ways to regulate glucose transporter 4. *Appl Physiol Nutr Metab*. 2009; 34: 481–7.
16. **Gruzman A, Babai G, Sasson S.** Adenosine monophosphate-activated protein kinase (AMPK) as a new target for antidiabetic drugs: a review on metabolic, pharmacological and chemical considerations. *Rev Diabet Stud*. 2009; 6: 13–36.
17. **Momcilovic M, Hong SP, Carlson M.** Mammalian TAK1 activates Snf1 protein kinase in yeast and phosphorylates AMP-activated protein kinase *in vitro*. *J Biol Chem*. 2006; 281: 25336–43.
18. **Woods A, Dickerson K, Heath R, *et al.*** Ca2+/calmodulin-dependent protein kinase kinase-beta acts upstream of AMP-activated protein kinase in mammalian cells. *Cell Metab*. 2005; 2: 21–33.
19. **Woods A, Johnstone SR, Dickerson K, *et al.*** LKB1 is the upstream kinase in the AMP-activated protein kinase cascade. *Curr Biol*. 2003; 13: 2004–8.
20. **Hayashi T, Hirshman MF, Fujii N, *et al.*** Metabolic stress and altered glucose transport: activation of AMP-activated protein kinase as a unifying coupling mechanism. *Diabetes*. 2000; 49: 527–31.
21. **Eguez L, Lee A, Chavez JA, *et al.*** Full intracellular retention of GLUT4 requires AS160 Rab GTPase activating protein. *Cell Metab*. 2005; 2: 263–72.
22. **Miinea CP, Sano H, Kane S, *et al.*** AS160, the Akt substrate regulating GLUT4 translocation, has a functional Rab GTPase-activating protein domain. *Biochem J*. 2005; 391: 87–93.
23. **Fujii N, Jessen N, Goodyear LJ.** AMP-activated protein kinase and the regulation of glucose transport. *Am J Physiol Endocrinol Metab*. 2006; 291: E867–77.
24. **Reznick RM, Zong H, Li J, *et al.*** Aging-associated reductions in AMP-activated protein kinase activity and mitochondrial biogenesis. *Cell Metab*. 2007; 5: 151–6.
25. **Lopaschuk GD.** AMP-activated protein kinase control of energy metabolism in the ischemic heart. *Int J Obes*. 2008; 32: S29–35.
26. **Russell RR, 3rd, Li J, Coven DL, *et al.*** AMP-activated protein kinase mediates ischemic glucose uptake and prevents postischemic cardiac dysfunction, apoptosis, and injury. *J Clin Invest*. 2004; 114: 495–503.
27. **Wang Y, Gao E, Tao L, *et al.*** AMP-activated protein kinase deficiency enhances myocardial ischemia/reperfusion injury but has minimal effect on the antioxidant/antinitrative protection of adiponectin. *Circulation*. 2009; 119: 835–44.
28. **Boyle JG, Salt IP, McKay GA.** Metformin action on AMP-activated protein kinase: a translational research approach to understanding a potential new therapeutic target. *Diabet Med*. 2010; 27: 1097–106.
29. **Lee JO, Lee SK, Jung JH, *et al.*** Metformin induces Rab4 through AMPK and modulates GLUT4 translocation in skeletal muscle cells. *J Cell Physiol*. 2010; 226: 974–81.
30. **Sajan MP, Bandyopadhyay G, Miura A, *et al.*** AICAR and metformin, but not exercise, increase muscle glucose transport through AMPK-, ERK-, and PDK1-dependent activation of atypical PKC. *Am J Physiol Endocrinol Metab*. 2010; 298: E179–92.
31. **Bikman BT, Zheng D, Kane DA, *et al.*** Metformin improves insulin signaling in obese rats *via* reduced IKKbeta action in a fiber-type specific manner. *J Obes*. 2010; doi:10.1155/2010/970865.
32. **Kane DA, Anderson EJ, Price JW, 3rd, *et al.*** Metformin selectively attenuates mitochondrial H2O2 emission without affecting respiratory capacity in skeletal muscle of obese rats. *Free Radic Biol Med*. 2010; 49: 1082–7.
33. **Arakawa M, Taketomi S, Furuno K, *et al.*** Metabolic studies on the development of ethanol-induced fatty liver in KK-Ay mice. *J Nutr*. 1975; 105: 1500–8.
34. **Iwatsuka H, Shino A, Suzuoki Z.** General survey of diabetic features of yellow KK mice. *Endocrinol Jpn*. 1970; 17: 23–35.
35. **Laguens RP, Candela S, Hernandez RE, *et al.*** Streptozotocin-induced liver damage in mice. *Horm Metab Res*. 1980; 12: 197–201.
36. **Levine BS, Henry MC, Port CD, *et al.*** Toxicologic evaluation of streptozotocin (NSC 85998) in mice, dogs and monkeys. *Drug Chem Toxicol*. 1980; 3: 201–12.